Electronic Supplementary Information

One-pot synthesis porous nanosphere $Ni_{0.85}Se$ on graphene as efficient and durable electrocatalyst for overall water splitting

Guigui Liu [a], Chao Shuai [a], Zunli Mo* [a], Ruibin Guo [a], Nijuan Liu [a], Xiaohui Niu [a], Qibing Dong [a], Jia Wang [a], Qinqin Gao [a], Ying Chen [a], Wentong Liu [a]

([a] Research Center of Gansu Military and Civilian Integration Advanced Structural Materials, Key Laboratory of Eco-Environment-Related Polymer Materials, Ministry of Education of China, Key Laboratory of Polymer Materials of Gansu Province, College of Chemistry and Chemical Engineering, Northwest Normal University, Lanzhou 730070, China)

* Corresponding author. Tel.: +86-13919467372

Email address: mozlnwnu@126.com

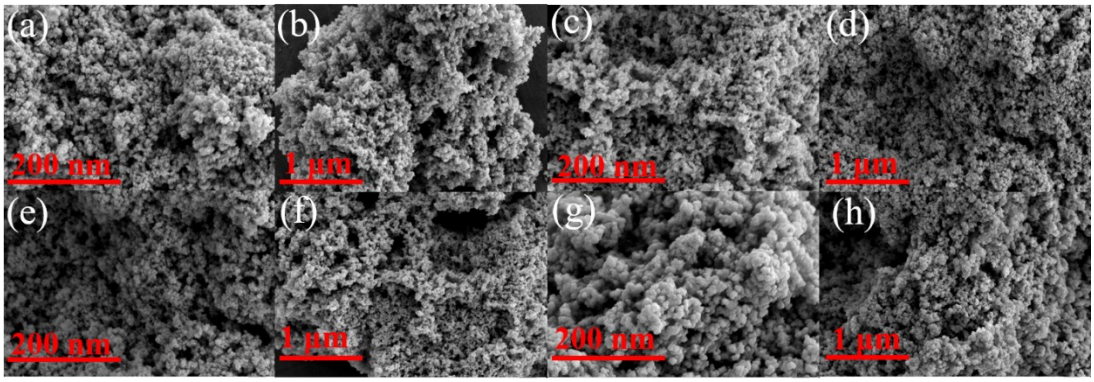

Figure S1. SEM images of $Ni_{0.85}Se$ under the different hydrothermal temperature conditions (with the hydrothermal time is 10 h): (a, b) 120 °C, (c, d) 160 °C, (e, f) 180 °C and (g, h) 200 °C.

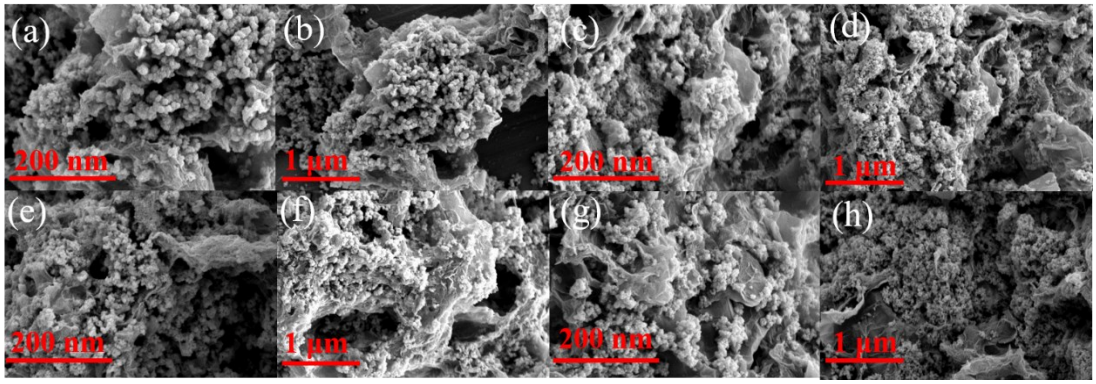

Figure S2. SEM images of $Ni_{0.85}Se$/RGO under the different hydrothermal temperature conditions (with the hydrothermal time is 10 h): (a, b) 120 °C, (c, d) 160 °C, (e, f) 180 °C and (g, h) 200 °C.

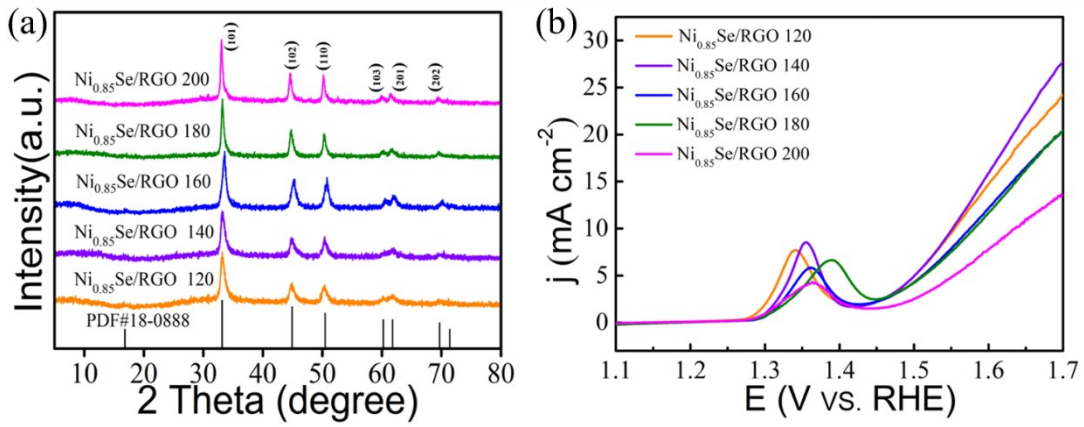

Figure S3. (a) The XRD patterns and (b) the polarization curves of the $Ni_{0.85}Se$/RGO in different temperature conditions (with the hydrothermal time is 10h).

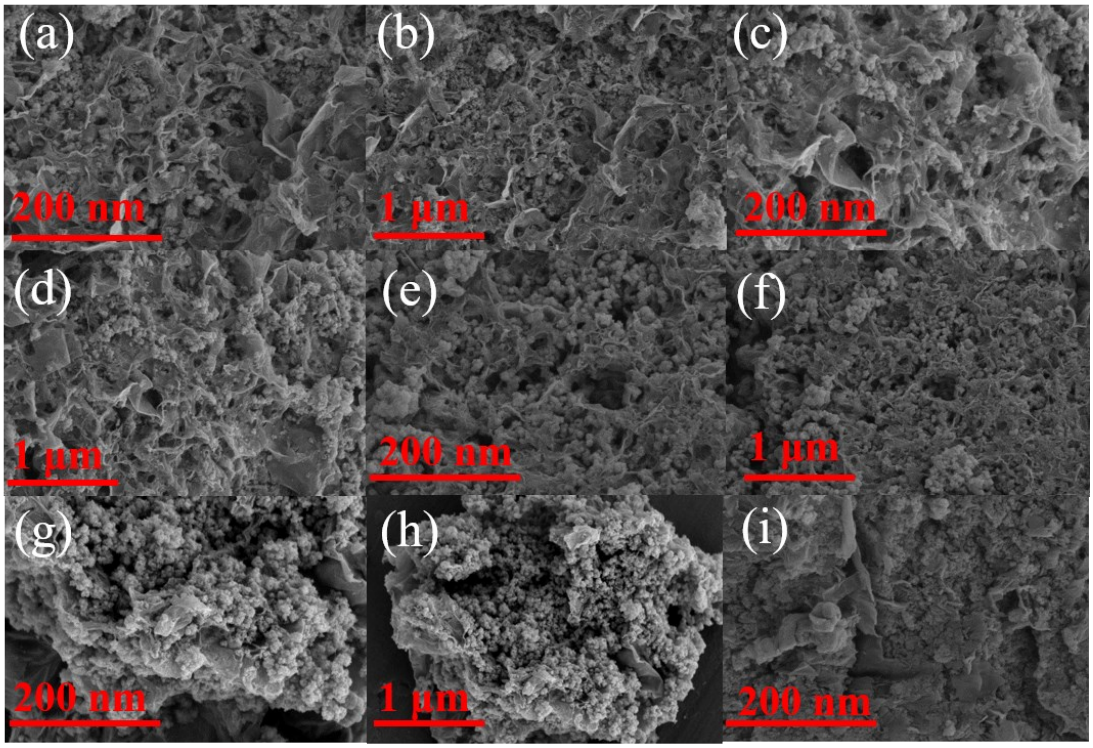

Figure S4. SEM images of $Ni_{0.85}Se$/RGO under the different hydrothermal time conditions (with the hydrothermal temperature is 140 °C): (a, b) 6 h, (c, d) 8 h, (e, f) 12 h, (g, h) 14 h and (i) 16 h.

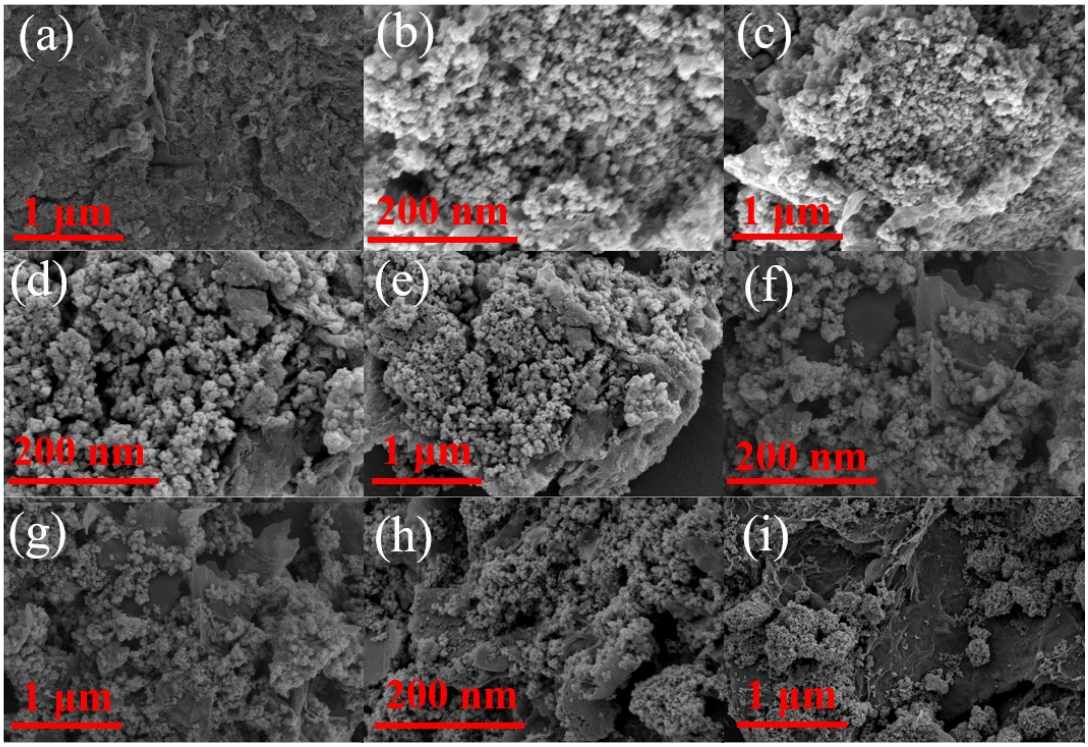

Figure S5. SEM images of $Ni_{0.85}Se$/RGO under the different hydrothermal time conditions (with the hydrothermal temperature is 140 °C): (a) 16 h, (b, c) 18 h, (d, e) 20 h, (f, g) 20 h and (i) 24 h.

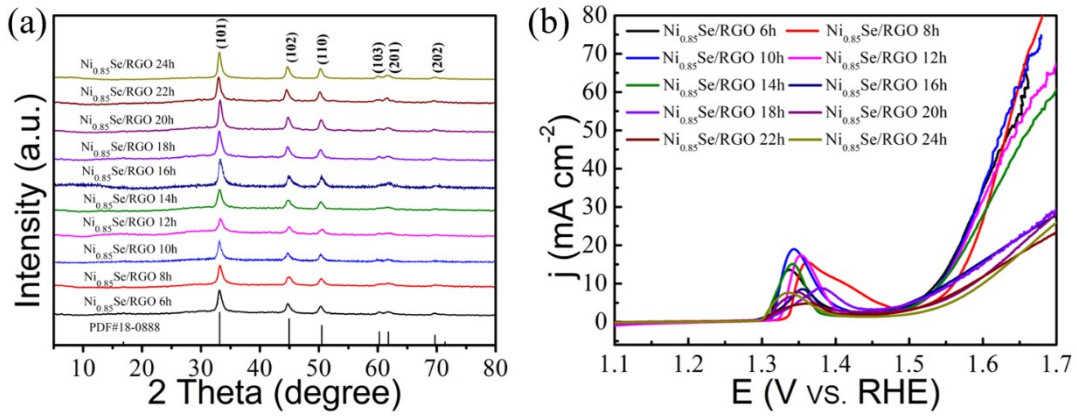

Figure S6. (a) The XRD patterns and the polarization curves of the $Ni_{0.85}Se$/RGO in different time conditions (with the hydrothermal temperature is 140 °C).

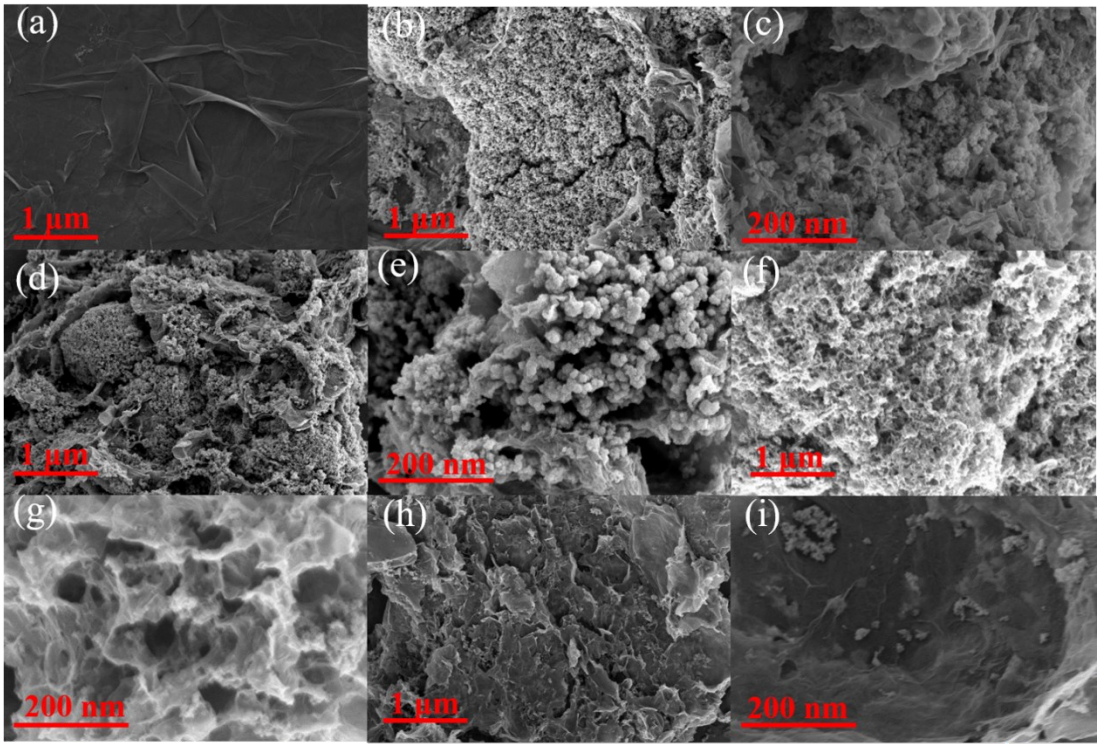

Figure S7. SEM images of $Ni_{0.85}Se$/RGO synthesized by varying the GO mass: (a) RGO, (b, c) $Ni_{0.85}Se$/RGO-1, (d, e) $Ni_{0.85}Se$/RGO-2, (f, g) $Ni_{0.85}Se$/RGO-4 and (h, i) $Ni_{0.85}Se$/RGO-5.

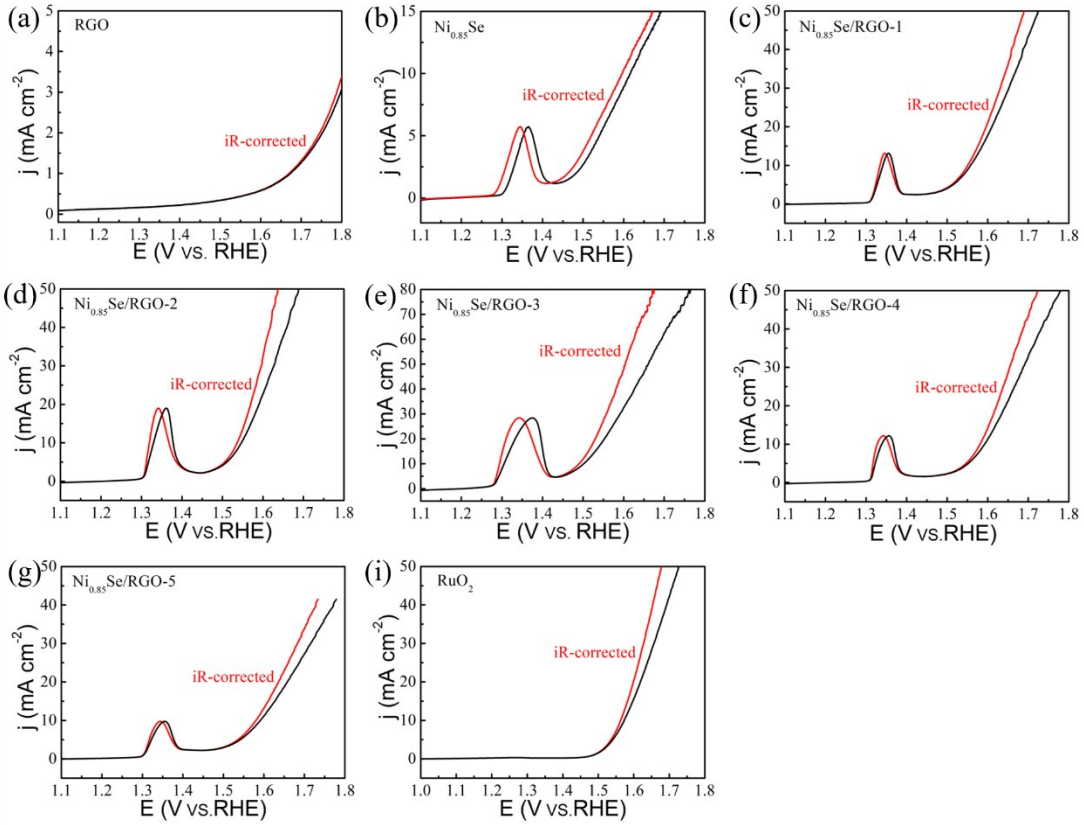

Figure S8. OER polarization curves of catalysts with and without iR compensation on GCE in 1.0 M KOH. The solution series resistances (R_s) were determined by the EIS, all of the catalysts show the similar R_s (~7 Ω).

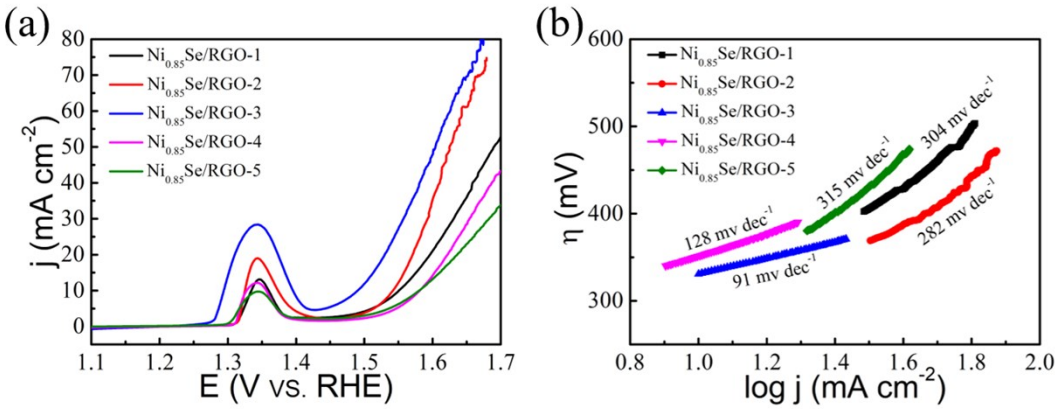

Figure S9. (a) the polarization curves and (b) Tafel plots derived from (a) of the various $Ni_{0.85}Se$/RGO composites.

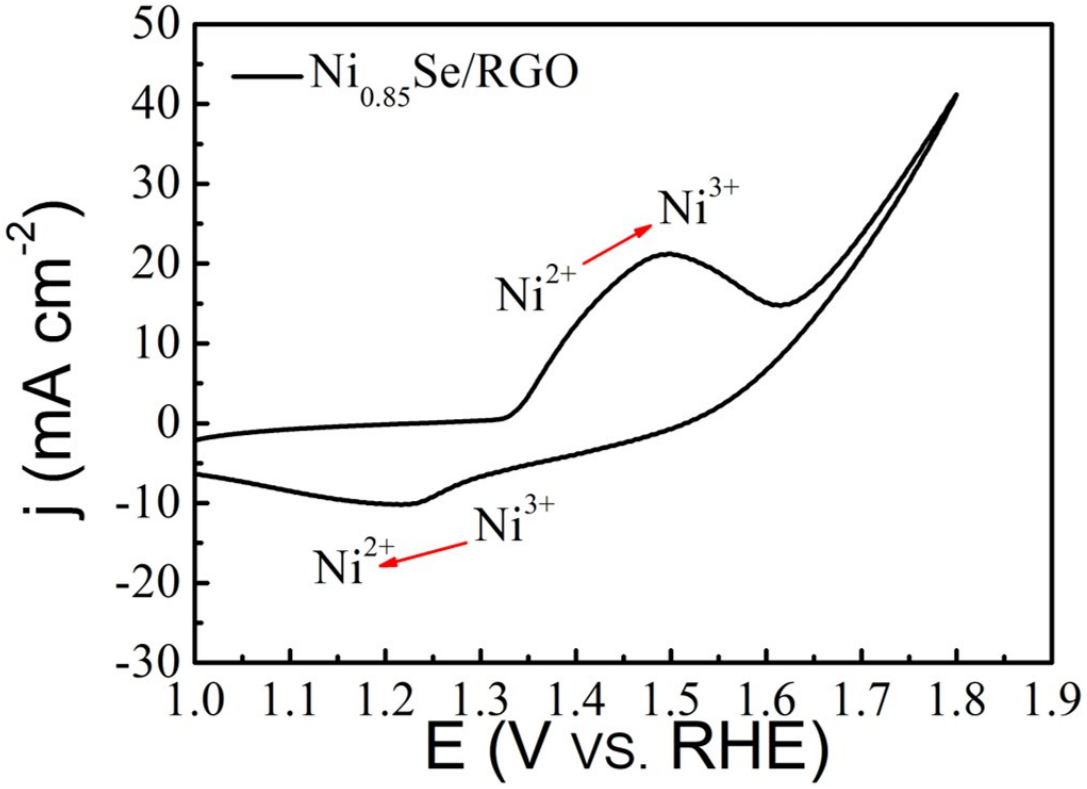

Figure S10. Cyclic voltammetry of $Ni_{0.85}Se$/RGO electrode.

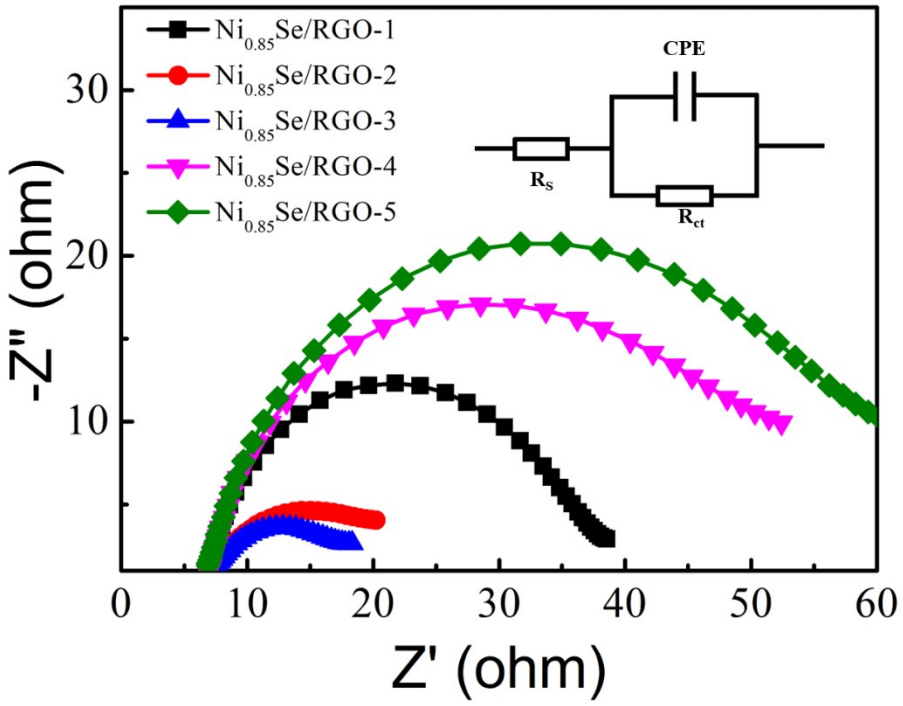

Figure S11. OER Nyquist plots of the various $Ni_{0.85}Se$/RGO composites at a potential of 1.42 V (vs. RHE), equivalent circuit model (the inset).

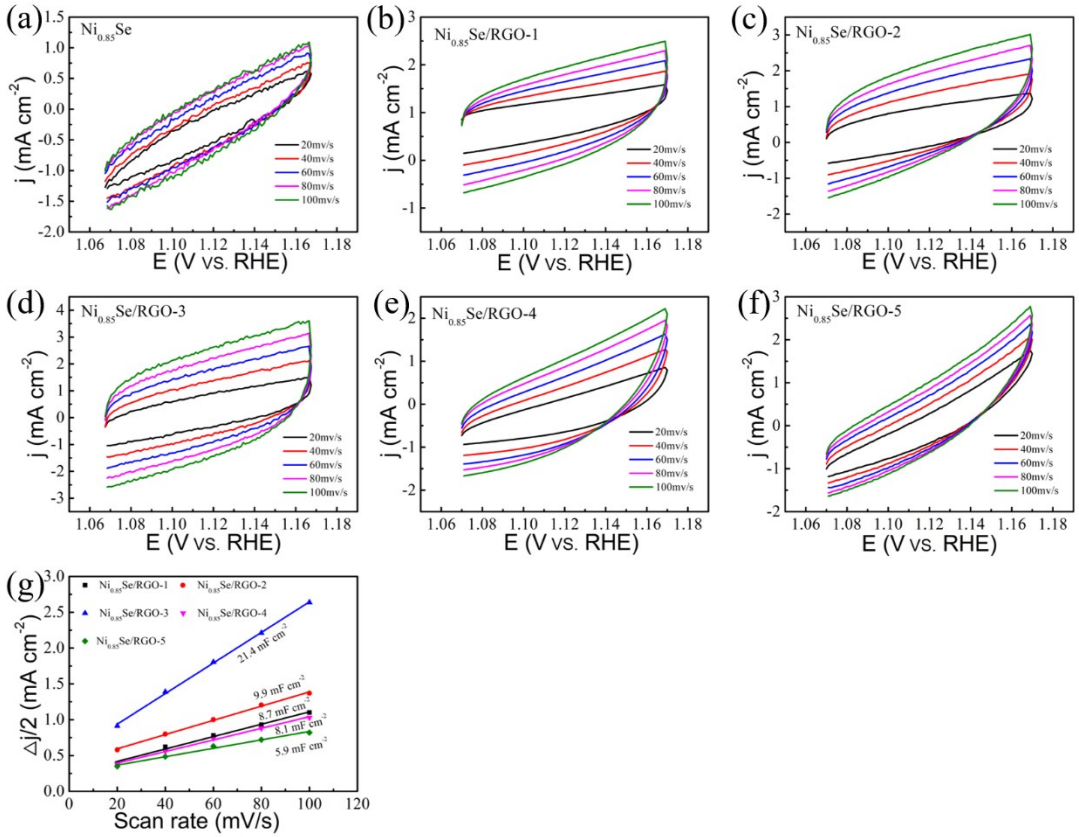

Figure S12. (a-f) Cyclic voltammograms at different scan rate for $Ni_{0.85}Se$ and the various $Ni_{0.85}Se$/RGO composites; (g) Capacitive currents at 1.12 mV vs. RHE of various $Ni_{0.85}Se$/RGO composites for electrocatalytic OER.

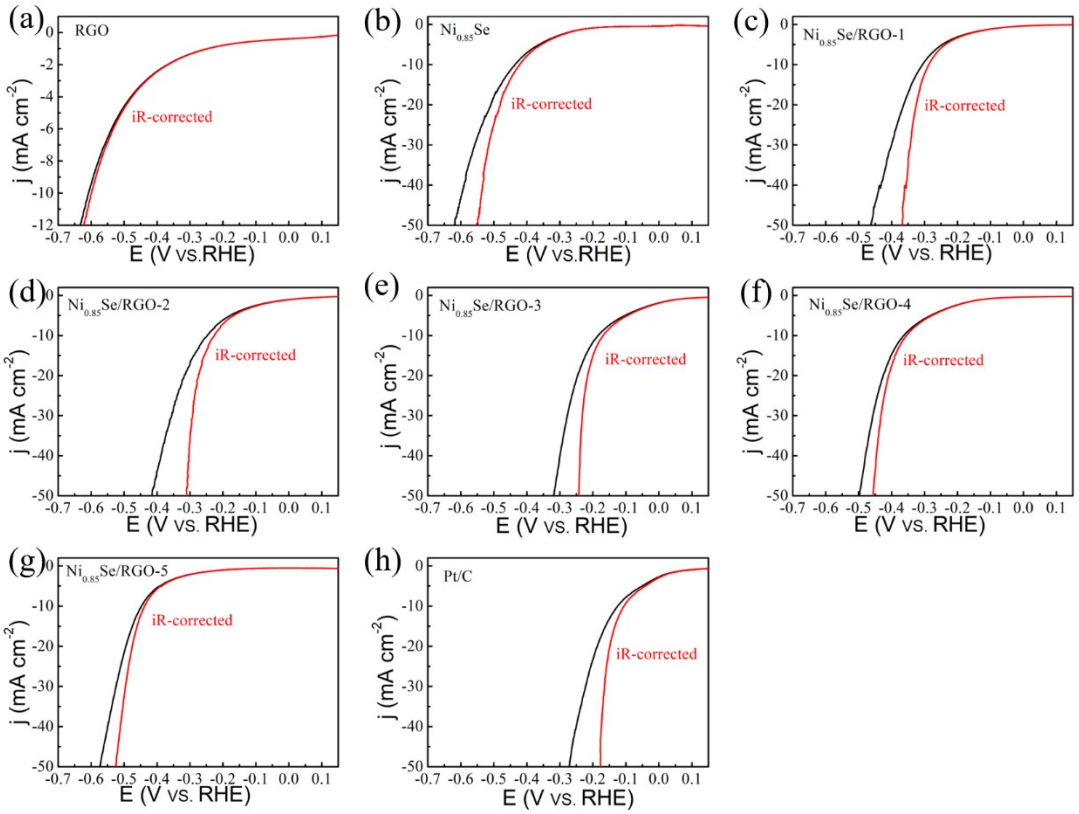

Figure S13. HER polarization curves of catalysts with and without iR compensation on GCE in 1.0 M KOH. The solution series resistances (R_s) were determined by the EIS, all of the catalysts show the similar R_s (~7 Ω).

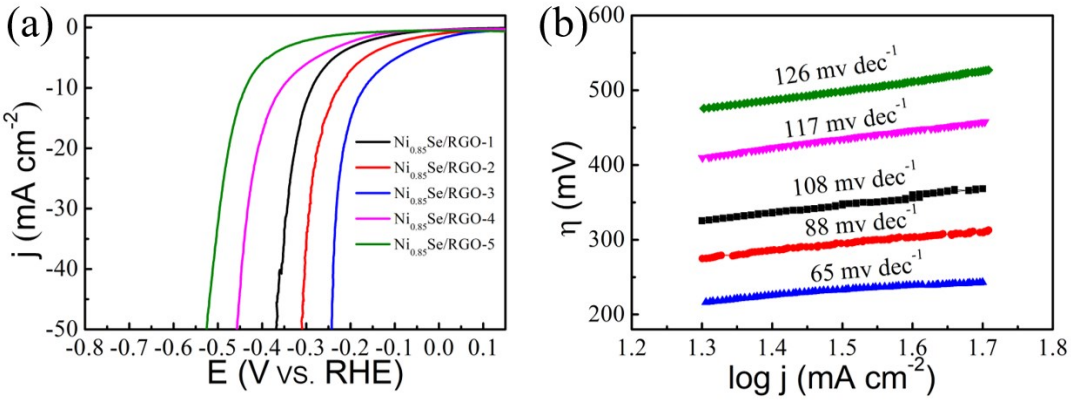

Figure S14. (a) the polarization curves and (b) Tafel plots derived from (a) of the various $Ni_{0.85}Se$/RGO composites.

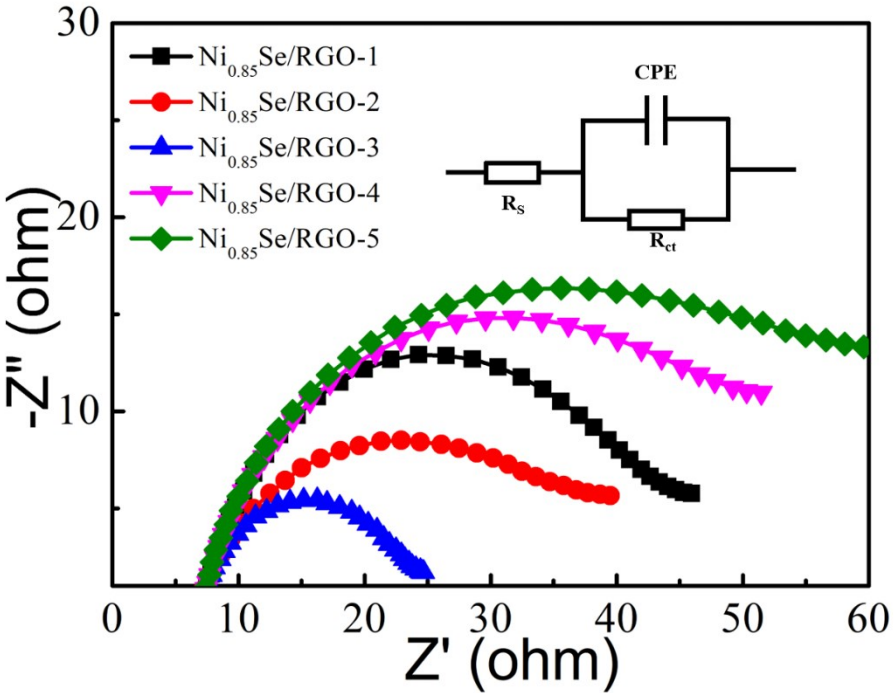

Figure S15. HER Nyquist plots of the various $Ni_{0.85}Se$/RGO composites at a potential of -0.35 V (vs. RHE), equivalent circuit model (the inset).

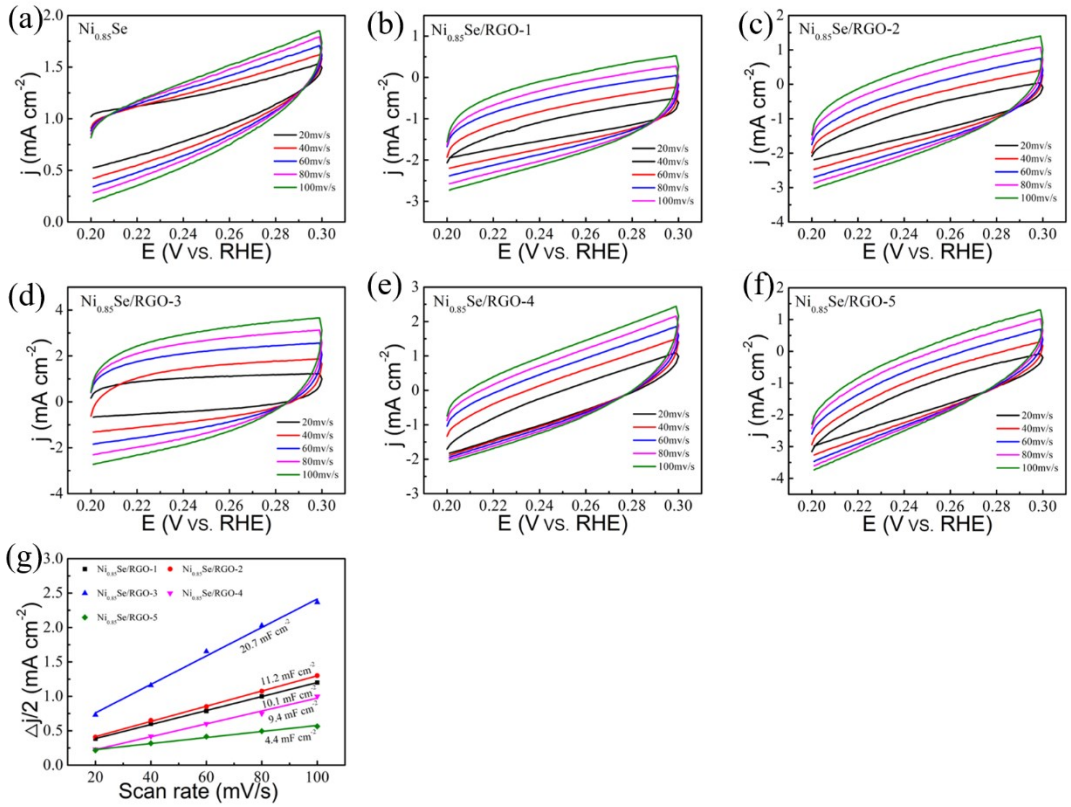

Figure S16. (a-f) Cyclic voltammograms at different scan rate for $Ni_{0.85}Se$ and the various $Ni_{0.85}Se$/RGO composites; (g) Capacitive currents at 0.25 mV vs. RHE of various $Ni_{0.85}Se$/RGO composites for electrocatalytic HER.

Calculation of activity and turnover frequency

Mass activity (J, A g^{-1}) and turnover frequency (TOF) were evaluated at an overpotential of η= 300 mV vs RHE.

The mass activity was calculated from the catalyst loading m (0.35 mg cm^{-2}) and the measured current density J (mA cm^{-2}).

$$\text{Mass activity} = J/m$$

Turnover frequency was calculated by the following equation:

$$TOF = (J \times A)/(4 \times F \times n)$$

Where J is the current density at a given overpotential, A is the surface area of the electrode, the number of 4 represents 4 electrons/mol of O_2, F is the Faraday constant (96485.3 C mol^{-1}), and n stands for the number of moles of Ni ions in $Ni_{0.85}Se$ and $Ni_{0.85}Se$/RGO [S3].

Table S1 Experimental conditions for the preparation of $Ni_{0.85}Se$/RGO Catalysts

Catalysts	$NiCl_2 \cdot 6H_2O$ (mg)	Se (mg)	GO (mg)
$Ni_{0.85}Se$/RGO-1	607	237	30
$Ni_{0.85}Se$/RGO-2	607	237	60
$Ni_{0.85}Se$/RGO-3	607	237	90
$Ni_{0.85}Se$/RGO-4	607	237	120
$Ni_{0.85}Se$/RGO-5	607	237	150

Table S2 Summary of OER performances of some catalysts in previous works.

catalysts	η (mV)	j (mA cm^{-2})	reference
$Ni_{0.85}Se$/RGO	30	320	This work
$Ni_{0.85}Se$	10	367	This work
$Ni_{0.85}Se$/GS	10	302	[S1]
Ti@$Ni_{0.85}Se$	30	270	[S2]
NiSe-$Ni_{0.85}Se$/CP	10	300	[S3]
Co_9S_8@MoS_2/CNF	10	430	[S4]
$Ni(OH)_2$	10	300	[S5]
N-graphene-CoO	10	340	[S6]
NiSe@NiOOH/NF	50	332	[S7]
$NiCo_2S_4$/RGO	10	366	[S8]
Ni@graphene	10	370	[S9]
$NixCo_{3-x}O_4$	10	420	[S10]

Table S3 Summary of HER performances of some catalysts in previous works.

catalysts	j (mA cm^{-2})	η (mV)	reference
$Ni_{0.85}Se$/RGO	10	169	This work
$Ni_{0.85}Se$	10	437	This work
$Ni_{0.85}Se$/GS	10	200	[S1]
Ti@$Ni_{0.85}Se$	30	120	[S2]
NiSe-$Ni_{0.85}Se$/CP	10	101	[S3]
Co_9S_8@MoS_2/CNF	10	190	[S4]
Ni_3S_2	10	223	[S11]
NiSe	10	187	[S12]
$NiSe_2$	40	200	[S13]
$NiSe_2$@NG	10	248	[S14]
Ni1Co1 – P	10	169	[S15]
$Ni_{0.85}Se$-SnO_2	25	290	[S16]

Table S4 Summary of overall water splitting performances of some catalysts in previous works.

catalysts	j (mA cm^{-2})	overall water splitting performance (V)	reference
$Ni_{0.85}Se$/RGO	10	1.64	This work
$Ni_{0.85}Se$/GS	10	1.7	[S1]
Ti@$Ni_{0.85}Se$	10	1.66	[S2]
NiSe-$Ni_{0.85}Se$/CP	10	1.62	[S3]
Mo-Ni_3S_2/NF	10	1.49	[S17]
Ni@NC	10	1.6	[S18]
NiFe/$NiCo_2O_4$/NF	10	1.67	[S19]

Note: GS, graphite substrate; CNF, carbon nanofibers; NF, Ni foam; CP, carbon fiber paper.

[S1] X. Wu, D. He, H. Zhang, H. Li, Z. Li, B. Yang, X. Zhang, $Ni_{0.85}Se$ as an efficient non-noble bifunctional electrocatalyst for full water splitting. International Journal of Hydrogen Energy, (2016) 10688-10694.

[S2] C. Yang, J. Zhang, G. Gao, D. Liu, R. Liu, R. Fan, Y. Wang, 3D Metallic Ti@$Ni_{0.85}Se$ with triple hierarchy as high-efficiency electrocatalyst for overall water splitting. ChemSusChem, (2019) 2271-2277.

[S3] Y. Chen, Z. Ren, H. Fu, X. Zhang, G. Tian, H. Fu, NiSe-$Ni_{0.85}Se$ heterostructure nanoflake arrays on carbon paper as efficient electrocatalysts for overall water splitting. Small, (2018) 1800763.

[S4] H. Zhu, J. Zhang, R. Yanzhang, M. Du, Q. Wang, When Cubic Cobalt Sulfide Meets Layered Molybdenum Disulfide: A Core–Shell System Toward Synergetic Electrocatalytic Water Splitting. Adv Mater. (2015) 4752-4759.

[S5] L-A. Stern, X. Hu, Enhanced oxygen evolution activity by NiO_x and $Ni(OH)_2$ nanoparticles. Faraday Discuss. (2014) 363-379

[S6] S. Mao, Z. Wen, T. Huang, Y. Hou, J. Chen, High-performance bi-functional electrocatalysts of 3D crumpled graphene-cobalt oxide nanohybrids for oxygen reduction and evolution reactions. Energy Environ Sci. (2014) 609-616.

[S7] X. Li, G. Q. Han, Y.R. Liu, B. Dong, W. H. Hu, X. Shang, C. G. Liu, NiSe@NiOOH coreshell hyacinth-like nanostructures on nickel foam synthesized by

in situ electrochemical oxidation as an efficient electrocatalyst for the oxygen evolution reaction. ACS applied materials & interfaces, (2016) 20057-20066.

[S8] C. Shuai, Z. L. Mo, X. H. Niu, X. Yang, G. G. Liu, J. Wang, N. J. Liu , R. B. Guo, Hierarchical $NiCo_2S_4$ nanosheets grown on graphene to catalyze the oxygen evolution reaction. Journal of Materials Science, 55(4), 1627-1636.

[S9] X. Li, G. Q. Han, Y. R. Liu, B. Dong, X. Shang, W. H. Hu, C. G. Liu, In situ grown pyramid structures of nickel diselenides dependent on oxidized nickel foam as efficient electrocatalyst for oxygen evolution reaction. Electrochimica Acta, (2016) 77-84.

[S10] Y. Li, P. Hasin, Y. Wu, $NixCo_{3-x}O_4$ nanowire arrays for electrocatalytic oxygen evolution. Advanced materials, (2010) 1926-1929.

[S11] L. L. Feng, G. Yu, Y. Wu, G. D. Li, H. Li, Y. Sun, T. Asefa, W. Chen, X. Zou, J. Am. Chem. Soc., (2015) 14023-14026.

[S12] C. Tang, N. Cheng, Z. Pu, W. Xing, X. Sun, Angew. Chem. Int. Ed, 2015, 54, 9351-9355.

[S13] B. Yu, X. Wang, F. Qi, B. Zheng, J. He, J. Lin, Y. Chen, Self-assembled coral-like hierarchical architecture constructed by $NiSe_2$ nanocrystals with comparable hydrogen-evolution performance of precious platinum catalyst. ACS Applied Materials & Interfaces, 9(8) (2017) 7154-7159.

[S14] W. Li, B. Yu, Y. Hu, X. Wang, D. Yang, Y. Chen, Core–Shell Structure of $NiSe_2$ Nanoparticles@ Nitrogen-Doped Graphene for Hydrogen Evolution Reaction in Both Acidic and Alkaline Media. ACS Sustainable Chemistry & Engineering, 7(4) (2019)

4351-4359.

[S15] C. Shuai, Z. Mo, X. Niu, P. Zhao, Q. Dong, Y. Chen, R. Guo, Nickel/cobalt bimetallic phosphides derived metal-organic frameworks as bifunctional electrocatalyst for oxygen and hydrogen evolution reaction. Journal of Alloys and Compounds, 847 (2020) 156514.

[S16] W. Hou, B. Zheng, F. Qi, J. He, W. Zhang, Y. Chen, Graphene wrapped self-assembled $Ni_{0.85}Se$-SnO_2 microspheres as highly efficient and stable electrocatalyst for hydrogen evolution reaction. Electrochimica Acta, 283 (2018) 1146-1153.

[S17] J. Li, Z. Yang, Y. Lin, J. Wang, F. Jiao, Y. Gong, Self-supported molybdenum doping Ni_3S_2 nanoneedles as efficient bifunctional catalysts for overall water splitting. New Journal of Chemistry, 20 (2020) 8578-8586.

[S18] Y. Xu, W. Tu, B. Zhang, S. Yin, Y. Huang, M. Kraft, R. Xu, Nickel Nanoparticles Encapsulated in Few‐Layer Nitrogen‐Doped Graphene Derived from Metal–Organic Frameworks as Efficient Bifunctional Electrocatalysts for Overall Water Splitting. Advanced Materials, 11 (2017) 1605957.

[S19] C. L. Xiao, Y. B. Li, X. Y. Lu, C. Zhao, Bifunctional porous NiFe/$NiCo_2O_4$/Ni foam electrodes with triple hierarchy and double synergies for efficient whole cell water splitting. Advanced Functional Materials, 20 (2016) 3515-3523.